Available online at www.sciencedirect.com
SCIENCE DIRECT®
Journal of Sound and Vibration 269 (2004) 489–509
JOURNAL OF SOUND AND VIBRATION
www.elsevier.com/locate/jsvi

Accessibility and identifiability of horizontal vibration in 3-D two-link flexible robots: system mode approach

Joono Cheong*, Youngil Youm, Wan Kyun Chung

Robotics and Biomechatronics Laboratory, Department of Mechanical Engineering, Pohang University of Science and Technology (POSTECH), San 31, Hyoja-dong, Pohang 790-784, South Korea

Received 2 April 2002; accepted 19 December 2002

Abstract

The accessibility of horizontal vibration in a 3-D two-link flexible robot shows configuration-dependent nature (International Journal of Robotics Research 16 (1997) 567). This paper deals with physical meaning of the accessibility issue in conjunction with system mode approach. The identifiability which is dual to the accessibility is also discussed. The analysis of horizontal vibration based on system mode approach takes an important role in examining the vibration accessibility. The ensuing Lagrangian dynamic formulation enables the formal definition of rigid–flexible coupled dynamic terms which show clear physical meaning. Both theoretical and numerical studies are presented to elucidate the meaning of the accessibility and the identifiability of horizontal vibration. In addition, the experimental results support the theoretical results.

1. Introduction

The use of flexible robot has a lot of advantages for particular needs: lightweight structures, low power consumption, safety for humans, and provision of passive compliance. The elastic structures bring about vibrations from the slender shapes of robot's links and their low stiffness. The vibrations must be compensated either by active control or by passive control to increase productivity. The modal feedback approach is one of the common control methods in suppressing vibration. Actual sensors (strain gauges or piezo films) measure vibrations that contain all the natural modes. If these sensors are distributed along the flexible body, the signals can be reconstructed into mode data by projecting onto mode shape functions. A finite number of sensors can determine a finite number of modes; there always exist unmeasured and uncontrolled

*Corresponding author. Tel.: +82-54-279-2844; fax: +82-84-279-5899.
E-mail address: jncheong@postech.ac.kr (J. Cheong).

0022-460X/03/$ - see front matter
doi:10.1016/S0022-460X(03)00008-7

residual modes [2]. It is important for the controller and the observer not to excite the residual modes [3]. The choice of the actuator position is another important factor in regard to vibration control. Every actuator in a system has its own actuator influence coefficient (AIC) that makes us guess the level of the controllability for vibration modes by that actuator. If the AIC of a certain mode is zero, the actuator cannot control the mode. Anyhow, if we would like to control the mode, we have two options to take: to re-place the actuator to other position or to change the robot structure in order that the AIC of the mode is non-zero [4,5]. The controllability and observability related with modal feedback of the flexible systems were studied by many authors, for example, Refs. [6–8].

In a PUMA-typed 3-D two-link flexible robot, shown in Fig. 1, the horizontal motion is defined only by the rotation of joint 1 (or base joint). The rotations of the other two joints constitute vertical motion. The vibration in the vertical plane is known to be controllable. On the other hand, the vibrations in the direction of horizontal motion are not always controllable. At certain configurations, some or all of the modes of horizontal vibration are uncontrollable. Tosunoglu et al. [9] and Konno et al. [1] examined this problem. They addressed the vibration controllability and accessibility by linearizing systems at a configuration and checked the rank of the controllability matrix. In addition, by neglecting Coriolis and centripetal force they quantify the level of controllability through accessibility index, which was conceptually similar to the magnitude of AIC. One thing they had missed is the physical meaning of those uncontrollable configurations.

The vibration controllability of flexible objects handled by rigid robots can be regarded as the same class of problems because once grasped, the payload is fixed to the robot body, and the

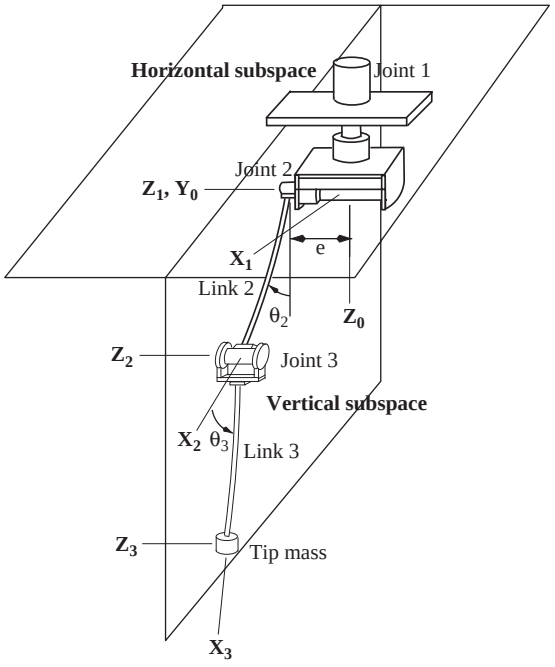

Fig. 1. Schematic of a 3-D two-link flexible robot.

robot becomes a flexible robot eventually. Zhou et al. [10] adopted the concept of vibration accessibility for evaluating the degree of the vibration controllability. Recently, the study on the measure for amount of vibration controllability in a redundant flexible robot depending on the configurations was reported [11].

In this paper, we focus on the accessibility and the identifiability of horizontal vibration for 3-D two-link flexible robots. We explore the physical meaning of the configurations where vibration modes are inaccessible and/or unidentifiable. We adopt system mode vibration analysis for interpreting the equations of motion, depending on configurations, in relation to rigid–flexible coupled dynamics; it was difficult to interpret the physical meaning of rigid–flexible coupled dynamics using the conventional component mode analysis due to the complexity of the involved modal terms. This paper is organized as follows: the preliminaries are presented in Section 2, the development of equation of horizontal motion using system mode approach is given in Section 3, and in Section 4, the accessibility and identifiability are dealt with. Finally, we make concluding remarks in Section 5.

2. Preliminaries

2.1. Equations of motion for general flexible robots

The assumed mode of each flexible member is to be combined with, whenever one formulates generic equations of motion for flexible systems. Every elastic component is modelled as series solutions with infinite degrees. Book [12] added the effect of flexibility to the extended homogenous transform matrix for flexible robots with articulated joints. He utilized an immediate co-ordinate for representing the internal motion due to the elastic deflections and rotations. If the clamped mode shapes are applied in modelling the elastic motion, the equations of motion for n-link flexible robot can be written as

$$\boldsymbol{M}(\boldsymbol{q})\ddot{\boldsymbol{q}} + \boldsymbol{C}(\boldsymbol{q},\dot{\boldsymbol{q}})\dot{\boldsymbol{q}} + \boldsymbol{K}\boldsymbol{q} + \boldsymbol{g}(\boldsymbol{q}) = \boldsymbol{B}\boldsymbol{\tau}, \tag{1}$$

that is,

$$\begin{bmatrix} \boldsymbol{M}_{rr}(\boldsymbol{q}) & \boldsymbol{M}_{rf}(\boldsymbol{q}) \\ \boldsymbol{M}_{fr}(\boldsymbol{q}) & \boldsymbol{M}_{ff}(\boldsymbol{q}) \end{bmatrix} \begin{bmatrix} \ddot{\boldsymbol{\theta}} \\ \ddot{\boldsymbol{v}} \end{bmatrix} + \begin{bmatrix} \boldsymbol{C}_{rr}(\boldsymbol{q},\dot{\boldsymbol{q}}) & \boldsymbol{C}_{rf}(\boldsymbol{q},\dot{\boldsymbol{q}}) \\ \boldsymbol{C}_{fr}(\boldsymbol{q},\dot{\boldsymbol{q}}) & \boldsymbol{C}_{ff}(\boldsymbol{q},\dot{\boldsymbol{q}}) \end{bmatrix} \begin{bmatrix} \dot{\boldsymbol{\theta}} \\ \dot{\boldsymbol{v}} \end{bmatrix} + \begin{bmatrix} \boldsymbol{0} & \boldsymbol{0} \\ \boldsymbol{0} & \boldsymbol{K}_{ff} \end{bmatrix} \begin{bmatrix} \boldsymbol{\theta} \\ \boldsymbol{v} \end{bmatrix} + \begin{bmatrix} \boldsymbol{g}_r(\boldsymbol{q}) \\ \boldsymbol{g}_f(\boldsymbol{q}) \end{bmatrix} = \begin{bmatrix} \boldsymbol{I} \\ \boldsymbol{0} \end{bmatrix} \boldsymbol{\tau}, \tag{2}$$

where r and f denote rigid and flexible parts, respectively. The generalized co-ordinate of the system is defined as

$$\boldsymbol{q} = [\theta_1 \cdots \theta_n \ v_{1,1} \cdots v_{1,m_1} \cdots v_{n,m_n}]^{\mathrm{T}} = [\boldsymbol{\theta}^{\mathrm{T}} \boldsymbol{v}^{\mathrm{T}}]^{\mathrm{T}} \in \mathbb{R}^{n+m},$$

where $\boldsymbol{\theta} \in \mathbb{R}^n$ is the joint variable, $\boldsymbol{v} \in \mathbb{R}^m$ is the flexible variable, and $v_{i,j}$ means the jth vibration mode of the ith link. Actually, $v_{i,j}$s are the component mode solutions, which will be explained in detail in the next section. $\boldsymbol{M}(\boldsymbol{q}) \in \mathbb{R}^{(n+m)\times(n+m)}$ is the inertia matrix, $\boldsymbol{C}(\boldsymbol{q},\dot{\boldsymbol{q}}) \in \mathbb{R}^{(n+m)\times(n+m)}$ is the

Coriolis and centripetal matrix, $\boldsymbol{K} \in \mathbb{R}^{(n+m)\times(n+m)}$ is the stiffness matrix, $\boldsymbol{g} \in \mathbb{R}^{n+m}$ is the gravity vector, $\boldsymbol{B} \in \mathbb{R}^{(n+m)\times n}$ is the input matrix, and $\boldsymbol{\tau} \in \mathbb{R}^n$ is the joint torque.

2.2. Modal accessibility

The vibration of a flexible robot sometimes cannot be controlled. This may result from the locations of actuators and the geometrical shapes of structures. Previous studies showed the configuration-dependent vibration controllability (or accessibility) of multi-link robots; see Refs. [1,9]. According to Ref. [1], in PUMA-typed 3-D two-link flexible robots there are sets of configurations where certain horizontal vibration modes are not controllable. To explore the linear vibration controllability, they reformulated Eq. (2) to get set-point regulation model by linearizing all the non-linear forces. As a background work of this paper, we briefly review the accessibility of vibration modes in multi-link systems, following the work in Ref. [1].

Consider a 3-D two-link flexible robot, shown in Fig. 1, whose geometric shape is determined by θ_2 and θ_3. If we assume that the motion of the robot has taken place at a stationary position $\boldsymbol{\theta} = \boldsymbol{\theta}_d$, the Coriolis and centripetal force is negligible. In addition, the dependency on flexure variables within inertia and gravity matrices becomes negligible, so that we get $\boldsymbol{M}(\boldsymbol{q}) = \boldsymbol{M}(\boldsymbol{\theta}_d)$, $\boldsymbol{g}(\boldsymbol{q}) = \boldsymbol{g}(\boldsymbol{\theta}_d)$. If we define

$$\begin{aligned} \tilde{\boldsymbol{v}} &\triangleq \boldsymbol{v} - \boldsymbol{K}_{ff}^{-1}\boldsymbol{g}_f(\boldsymbol{\theta}_d), \\ \tilde{\boldsymbol{\tau}} &\triangleq \boldsymbol{\tau} - \boldsymbol{g}_r(\boldsymbol{\theta}_d), \end{aligned} \tag{3}$$

then, we can get a linearized dynamic equation from Eq. (2) as

$$\begin{bmatrix} \ddot{\boldsymbol{\theta}} \\ \dot{\tilde{\boldsymbol{v}}} \end{bmatrix} = -\begin{bmatrix} \boldsymbol{H}_{rr}(\boldsymbol{\theta}_d) & \boldsymbol{H}_{rf}(\boldsymbol{\theta}_d) \\ \boldsymbol{H}_{fr}(\boldsymbol{\theta}_d) & \boldsymbol{H}_{ff}(\boldsymbol{\theta}_d) \end{bmatrix} \left(\begin{bmatrix} \boldsymbol{0} & \boldsymbol{0} \\ \boldsymbol{0} & \boldsymbol{K}_{ff} \end{bmatrix} \begin{bmatrix} \boldsymbol{\theta} \\ \tilde{\boldsymbol{v}} \end{bmatrix} - \begin{bmatrix} \tilde{\boldsymbol{\tau}} \\ \boldsymbol{0} \end{bmatrix} \right), \tag{4}$$

where

$$\begin{bmatrix} \boldsymbol{H}_{rr}(\boldsymbol{\theta}_d) & \boldsymbol{H}_{rf}(\boldsymbol{\theta}_d) \\ \boldsymbol{H}_{fr}(\boldsymbol{\theta}_d) & \boldsymbol{H}_{ff}(\boldsymbol{\theta}_d) \end{bmatrix} = \begin{bmatrix} \boldsymbol{M}_{rr}(\boldsymbol{\theta}_d) & \boldsymbol{M}_{rf}(\boldsymbol{\theta}_d) \\ \boldsymbol{M}_{fr}(\boldsymbol{\theta}_d) & \boldsymbol{M}_{ff}(\boldsymbol{\theta}_d) \end{bmatrix}^{-1}.$$

The lower part of the above equation denotes the motion of vibration. We make modal transformation to this part satisfying

$$\boldsymbol{\Phi}^{-1}(\boldsymbol{H}_{ff}\boldsymbol{K}_{ff})\boldsymbol{\Phi} = \boldsymbol{\Omega}, \tag{5}$$

where $\boldsymbol{\Omega} \in \mathbb{R}^{m\times m}$ is the diagonal eigenvalue matrix and $\boldsymbol{\Phi} \in \mathbb{R}^{m\times m}$ is the eigenvector matrix. Then, $\tilde{\boldsymbol{v}}$ can be expressed by the linear combination of the eigenvectors as

$$\tilde{\boldsymbol{v}} = \boldsymbol{\Phi}\boldsymbol{\eta},$$

where $\boldsymbol{\eta} \in \mathbb{R}^m$ is the modal co-ordinate. The transformed vibration equation becomes

$$\ddot{\boldsymbol{\eta}} = -\boldsymbol{\Omega}\boldsymbol{\eta} + \boldsymbol{\Gamma}\tilde{\boldsymbol{\tau}}, \tag{6}$$

where $\boldsymbol{\Gamma} = \boldsymbol{\Phi}^{-1}\boldsymbol{H}_{fr} \in \mathbb{R}^{m\times n}$. According to Ref. [1], if the row of $\boldsymbol{\Gamma}$ has a non-zero entry, the corresponding vibration mode is accessible. The level of accessibility of the ith mode at a $\boldsymbol{\theta}_d$ is

defined as

$$a_i(\boldsymbol{\theta}_d) = \sqrt{\boldsymbol{\gamma}_i \boldsymbol{\gamma}_i^{\mathrm{T}}},$$

where $\boldsymbol{\gamma}_i$ is the ith row vector of $\boldsymbol{\Gamma}$. If $a_i(\boldsymbol{\theta}_d)$ happens to be zero, the ith mode cannot be controlled by the actuator input. Over the whole space of joint configurations, we could notice singularity lines where a_is are zero. The inaccessible modes appeared always in horizontal vibration of the robot. Consequently, we must avoid the singular configurations as the final postures after horizontal movements.

The physical meaning of those inaccessible configurations remains unanswered as far as the authors' knowledge goes. It should be answered for better control, and to know the internal physics is the fundamental step. The aim of the present paper is, therefore, to prepare an answer for the question, which is very affirmative and has clear physical interpretation.

3. Horizontal dynamic equation: system mode approach

For deriving dynamic equations, the first thing to do is to determine the series solutions of mathematical vibration model. The vibrations of links in the most flexible robots have been modelled by the assumed component mode solutions as mentioned before. For illustration of component modes, consider the horizontal deflections of 3-D two-link flexible robot depicted in Fig. 2. The horizontal vibrations are defined from the roots of elastic links. In the component mode description, the natural frequencies and mode shapes are obtained by solving the assumed mode of each link independently without considering the other links. Thus, the component mode description is a well-known and conventional method for modelling vibration of flexible robots. By combining all the modal solutions of every link, the equations of motion for the total system will be obtained [12]. These solutions are included into kinematic and dynamic modelling. The degrees of freedom of a system with accurate model could be quite large. In many cases, we need

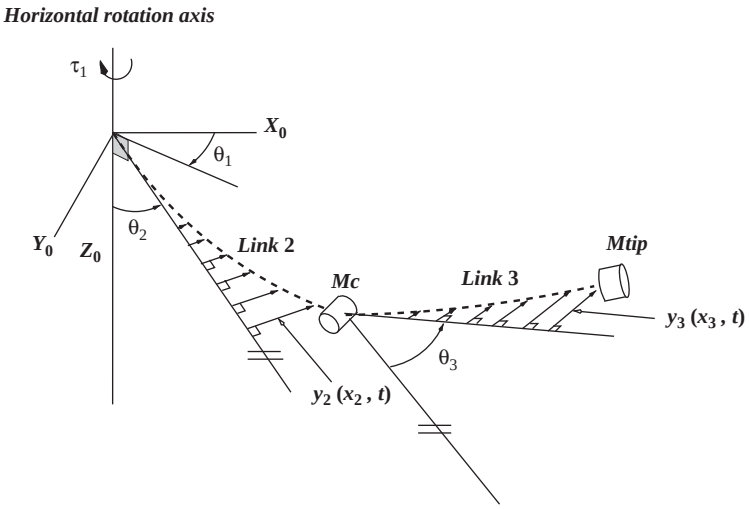

Fig. 2. Horizontal vibration in a 3-D two-link flexible robot: component mode approach.

model reduction in order to make the system manageable both for controller and for observer design. The initial step to this is the eigenvalue decomposition of whole dynamics. This will result in synthesized modes which represent the vibration modes of whole body [13,14]. Then, the higher modes will be removed, regarding the bandwidth of the system (plant, actuator, sensor, etc.) or other kinds of reduction criteria.

Another way of modelling the vibration is the system mode approach [15–17]. According to this approach, the natural modes are obtained by considering all the flexible links as one connected flexible structure. We do not reduce the original system into simpler pieces like the component mode approach. To solve the system modes, a set of partial differential equations (PDEs) for all the flexible elements is solved simultaneously with every boundary condition. The natural modes from the system mode approach are thus related to the whole body. The approach produces exact modes without matrix eigenvalue decomposition. Different from the vibration defined in Fig. 2, the horizontal vibration is defined by the deviation from the rigid configuration of whole body as shown in Fig. 3. The modal frequencies and mode shapes of system modes contain the elastic properties of the overall structure. One advantage of the system mode method is that there is no need to incorporate large dimensional vibration modes. Since the system mode offers the exact vibration modes of whole body, one can apply just the required amount of lower modes. This removes the model reduction procedure, which is a difficult step in assumed mode method. Another advantage is that it is useful for viewing the rigid–flexible interactive properties of dynamics when the equation of motion is constructed using exact system mode solutions. As far as the authors' knowledge goes, the dynamic equations for flexible robots with system modes have not been tried before. Thus, in this section, after a brief explanation on the system mode analysis on horizontal vibration of 3-D two-link flexible robot [17], the equations of motion will be

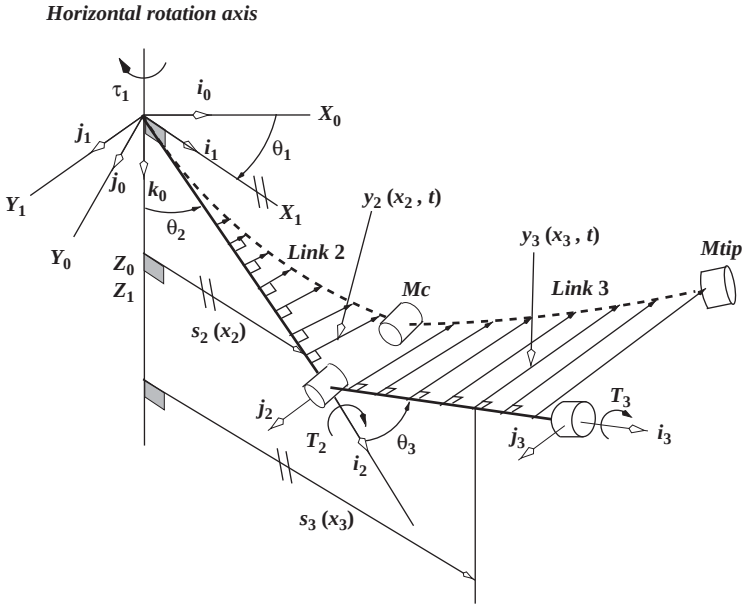

Fig. 3. Horizontal vibration in a 3-D two-link flexible robot: system mode approach.

formulated by using the results of system mode analysis. The resulting equations will provide an essential perspective to examining the accessibility and the identifiability of flexible systems.

3.1. System mode analysis for horizontal vibration

Consider a two-link flexible robot in Fig. 3, fixed at a configuration. Link 2 and Link 3 represent the first and the second elastic link, respectively. The horizontal bending vibration of two flexible links can be represented by the constrained PDEs:

$$EI_2 \frac{\partial^4 y_2(x_2,t)}{\partial x_2^4} + \rho_2 \ddot{y}_2(x_2,t) = 0,$$
$$EI_3 \frac{\partial^4 y_3(x_3,t)}{\partial x_3^4} + \rho_3 \ddot{y}_3(x_3,t) = 0, \tag{7}$$

where EI_i and ρ_i means, respectively, flexural rigidity and mass density of Link i in the horizontal direction, which are constant along the side of each link. The effect of torsional vibration, accompanied by the horizontal vibration, is described by

$$GJ_2 \frac{\partial^2 T_2(x_2,t)}{\partial x_2^2} - b_2 \ddot{T}_2(x_2,t) = 0,$$
$$GJ_3 \frac{\partial^2 T_3(x_3,t)}{\partial x_3^2} - b_3 \ddot{T}_3(x_3,t) = 0, \tag{8}$$

where T_i is the torsional deflection of Link i. GJ_i and b_i are the torsional rigidity and polar moment of inertia per unit length of Link i, respectively. The horizontal bending vibration $y(x,t)$ for whole body can be expressed by patching the solutions of $y_2(x_2,t)$ and $y_3(x_3,t)$ such that

$$y(x,t) = \begin{cases} y_2(x_2,t) = \sum_{j=1}^{m} \phi_{2j}(x_2) z_j(t), & 0 \leqslant (x = x_2) \leqslant L_2, \\ y_3(x_3,t) = \sum_{j=1}^{m} \phi_{3j}(x_3) z_j(t), & 0 \leqslant (x - L_2 = x_3) \leqslant L_3, \end{cases} \tag{9}$$

where ϕ_{ij} represents the jth system mode solution of Eq. (7) for Link i section, and $z_j(t)$ is the jth time solution. L_2 and L_3 are the lengths of Link 2 and Link 3, respectively. As for the torsional vibration, since the majority of torsional vibration occurs in the inner link, it is reasonable to assume that $T_3(x_3,t) \equiv 0$. Thus,

$$T(x,t) = \begin{cases} T_2(x_2,t) = \sum_{j=1}^{m} \eta_j(x_2) z_j(t), & 0 \leqslant (x = x_2) \leqslant L_2, \\ T_3(x_3,t) = 0, & 0 \leqslant (x - L_2 = x_3) \leqslant L_3, \end{cases} \tag{10}$$

where η_j is the jth system mode shape for torsional vibration of Link 2 section. If we perform the separation of variables by utilizing the normal mode time solution as

$$z_j(t) = \exp(\omega_j t), \tag{11}$$

we get ordinary differential equations (ODEs) for bending and torsional vibration such that

$$\frac{\mathrm{d}^4\phi_{ij}(x_i)}{\mathrm{d}x_2^4} - \lambda_{ij}^4\phi_{ij}(x_i) = 0, \quad i = 2,3, \quad j = 1,\ldots,m,$$
$$\frac{\mathrm{d}^2\eta_j(x_2)}{\mathrm{d}x_2^2} + \kappa_j^2\eta_j(x_2) = 0, \quad j = 1,\ldots,m, \tag{12}$$

where $\lambda_{ij}^4 \triangleq \rho_i\omega_j^2/EI_i$ and $\kappa_j^2 \triangleq b_2\omega_j^2/GJ_2$. The corresponding solutions can be given in the following forms:

$$\phi_{ij}(x_i) = A_i\sin(\lambda_{ij}x_i) + B_i\sinh(\lambda_{ij}x_i) + C_i\cos(\lambda_{ij}x_i) + D_i\cosh(\lambda_{ij}x_i),$$
$$\eta_j(x_2) = A_4\sin(\kappa_j x_2) + B_4\cos(\kappa_j x_2). \tag{13}$$

The boundary conditions at the joint is simply considered as the clamped end. Thus, we have

$$y_2(0,t) = 0, \quad y_2'(0,t) = 0, \quad T_2(0,t) = 0, \tag{14}$$

where $(\cdot)'$ means spatial derivative with respect to considered variable. At the elbow mass, the following are satisfied:

$$y_2(L_2,t) = y_3(0,t),$$
$$y_2'(L_2,t) - T_2(L_2,t)\sin\theta_3 = y_3'(0,t),$$
$$EI_2y_2''(L_2,t) = EI_3y_3''(0,t) - I_c\ddot{y}_2'(L_2,t),$$
$$EI_2y_2'''(L_2,t) = M_c\ddot{y}_2(L_2,t) + EI_3y_3'''(0,t),$$
$$GJ_2T_2'(L_2,t) = J_c\ddot{T}_2(L_2,t), \tag{15}$$

where I_c is the mass moment of inertia for elbow mass in $\boldsymbol{k}_2 = \boldsymbol{i}_2 \times \boldsymbol{j}_2$ direction shown in Fig. 3, J_c is the moment of inertia of the total outer body from the center in the direction of the torsional moment, and M_c denotes the elbow mass. In Eq. (15), the first two conditions are position and slope continuity, the third and fourth mean bending moment and shear force balances, and the last condition is the torsional moment balance. At the tip of the robot, there are two more boundary conditions:

$$EI_3y_3''(L_3,t) = -I_{tip}\ddot{y}_3'(L_3,t),$$
$$EI_3y_3'''(L_3,t) = M_{tip}\ddot{y}_3(L_3,t), \tag{16}$$

where I_{tip} and M_{tip} denote inertia and mass of tip element, respectively. Eq. (16) corresponds to the moment balance and shear force balance. Substituting Eqs. (11) and (13) into boundary conditions in Eqs. (14)–(16), we obtain linear equations as

$$\boldsymbol{H}(\omega_j)\boldsymbol{x} = \boldsymbol{0}, \tag{17}$$

where $\boldsymbol{x} = [A_2\ B_2\ C_2\ D_2\ A_3\ B_3\ C_3\ D_3\ A_4\ B_4]^{\mathrm{T}}$ is a vector of undetermined constant. The eigenvalues (or natural frequencies) of whole system are the solutions of the frequency equation given by

$$\det(\boldsymbol{H}(\omega_j)) = 0. \tag{18}$$

For the determined solutions, non-trivial $\boldsymbol{x}$'s, which are called eigenvectors, will be obtained in the null space of $\boldsymbol{H}(\omega_j)$. In the subsequent development, suppose that the solutions of Eq. (18) are

distinct. The imposition of all the boundary conditions offers us a useful orthogonal relation as follows:

$$\int_0^{L_2} \rho_2\phi_{2i}(x_2)\phi_{2j}(x_2)\,\mathrm{d}x_2 + \int_0^{L_3} \rho_3\phi_{3i}(x_3)\phi_{3j}(x_3)\,\mathrm{d}x_3 + \int_0^{L_2} b_2\eta_i(x_2)\eta_j(x_2)\,\mathrm{d}x_2 + M_c\phi_{2i}(L_2)\phi_{2j}(L_2) + I_c\phi'_{2i}(L_2)\phi'_{2j}(L_2) + M_{tip}\phi_{3i}(L_3)\phi_{3j}(L_3) + I_{tip}\phi'_{3i}(L_3)\phi'_{3j}(L_3) + J_c\eta_i(L_2)\eta_j(L_2) = 0 \quad \text{if } i \neq j. \tag{19}$$

For the proof, refer to Ref. [17]. Further, if we neglect the terms of the first-order derivative in Eq. (19) since I_c and I_{tip} are considerably small, we can rewrite Eq. (19) in a more compact form:

$$\oint_{D_2} \rho_2\phi_{2i}(x_2)\phi_{2j}(x_2)\,\mathrm{d}x_2 + \oint_{D_3} \rho_3\phi_{3i}(x_3)\phi_{3j}(x_3)\,\mathrm{d}x_3 + \oint_{D_2} b_2\eta_i(x_2)\eta_j(x_2)\,\mathrm{d}x_2 = 0 \quad \text{if } i \neq j, \tag{20}$$

where $\oint$ means the integral which includes lumped elements. D_2 and D_3 denote the appropriate integral domains in Link 2 and Link 3, respectively. If i and j are equal, we normalize the integral value in Eq. (20) as unity.

3.2. Lagrangian dynamic equation

We consider the Lagrangian dynamics associated with horizontal motion of a 3-D two-link flexible robot applying the system mode solutions. Since we deal with only the horizontal motion, θ_2 and θ_3 are regarded as geometric parameters. However, they will appear in the symbolic equation in order for us to change the value easily. The vertical deflection due to the gravity force is neglected as if the stiffness were infinite in vertical direction. Let $\boldsymbol{i}_0$, $\boldsymbol{j}_0$, and $\boldsymbol{k}_0$ be the unit vectors with respect to inertial frame $\{X_0, Y_0, Z_0\}$. And let a frame $\{X_1, Y_1, Z_1\}$ be a body fixed co-ordinate with unit vectors $\boldsymbol{i}_1$, $\boldsymbol{j}_1$, and $\boldsymbol{k}_1$ as shown in Fig. 3. We define $\boldsymbol{i}_i$, $i = 2, 3$, as a unit vector to outward direction of the ith link attached at the body, and $\boldsymbol{j}_i$, $i = 2, 3$, as a unit vector normal to the plane containing $\boldsymbol{i}_i$ and $\boldsymbol{k}_0$ vectors. Mathematically, it can be written that $\boldsymbol{j}_i = (\boldsymbol{k}_0 \times \boldsymbol{i}_i)/\|\boldsymbol{k}_0 \times \boldsymbol{i}_i\|$. Hence, $\boldsymbol{k}_i$, $i = 2, 3$, is defined as the common normal to both $\boldsymbol{i}_i$ and $\boldsymbol{j}_i$ according to right-hand co-ordinate convention. The position vector at a point of Link 2 can be written as

$$\boldsymbol{r}_2(x_2, t) = x_2\boldsymbol{i}_2 + y_2(x_2, t)\boldsymbol{j}_2, \tag{21}$$

where x_2 is the distance from the root of Link 2 to the point of interest. The second term is the elastic deflection, moving in the horizontal direction. Similarly, the position vector to a point of Link 3 can be written as

$$\boldsymbol{r}_3(x_3, t) = L_2\boldsymbol{i}_2 + x_3\boldsymbol{i}_3 + y_3(x_3, t)\boldsymbol{j}_3, \tag{22}$$

where x_3 is the distance from the root of Link 3 to the point of interest. With the help of the vibration described by system modes, $\boldsymbol{r}_3$ could be represented in a concise form. The velocities of $\boldsymbol{r}_2$ and $\boldsymbol{r}_3$ are

$$\dot{\boldsymbol{r}}_2(x_2, t) = \dot{\boldsymbol{r}}_2(x_2, t)^B + \theta_1\boldsymbol{k}_0 \times \boldsymbol{r}_2(x_2, t),$$
$$\dot{\boldsymbol{r}}_3(x_3, t) = \dot{\boldsymbol{r}}_3(x_3, t)^B + \theta_1\boldsymbol{k}_0 \times \boldsymbol{r}_3(x_3, t), \tag{23}$$

where

$$\dot{\boldsymbol{r}}_2^B(x_2,t) = \dot{y}_2(x_2,t)\boldsymbol{j}_2,$$
$$\dot{\boldsymbol{r}}_3^B(x_3,t) = \dot{y}_3(x_3,t)\boldsymbol{j}_3$$

mean the time derivatives of $\boldsymbol{r}_2(x_2,t)$ and $\boldsymbol{r}_3(x_3,t)$ with respect to body fixed frame. The cross-product between position and velocity yields angular momentum:

$$\begin{aligned}\boldsymbol{H}_\delta &= J_1\dot{\theta}_1\boldsymbol{k}_0 + \oint_{D_2} \boldsymbol{r}_2 \times \dot{\boldsymbol{r}}_2 \,\mathrm{d}m_2 + \oint_{D_3} \boldsymbol{r}_3 \times \dot{\boldsymbol{r}}_3 \,\mathrm{d}m_3 \\ &= J_1\dot{\theta}_1\boldsymbol{k}_0 + \sum_{i=2}^{3} \oint_{D_i} \boldsymbol{r}_i \times \dot{\boldsymbol{r}}_i \,\mathrm{d}m_i, \end{aligned} \tag{24}$$

where J_1 is the rotor inertia of joint 1. It can be further written that

$$\sum_{i=2}^{3} \oint_{D_i} \boldsymbol{r}_i \times \dot{\boldsymbol{r}}_i \,\mathrm{d}m_i = \sum_{i=2}^{3} \oint_{D_i} (\boldsymbol{r}_i \times \boldsymbol{j}_i)\dot{y}_i(x_i,t)\,\mathrm{d}m_i + \sum_{i=2}^{3} \dot{\theta}_1 \mathrm{II}_i \cdot \boldsymbol{k}_0, \tag{25}$$

since

$$\sum_{i=2}^{3} \oint_{D_i} \boldsymbol{r}_i \times (\dot{\theta}_1\boldsymbol{k}_0 \times \boldsymbol{r}_i)\,\mathrm{d}m_i = \sum_{i=2}^{3} \dot{\theta}_1 \mathrm{II}_i \cdot \boldsymbol{k}_0,$$

where II_i is the inertia tensor of the ith link. The first term on the right side of Eq. (25) is the angular momentum with respect to the body fixed frame, called modal angular momentum [18].

The kinetic energy of the considered two-link flexible robot can be written

$$\mathscr{T} = \frac{1}{2}J_1\dot{\theta}_1^2 + \sum_{i=2}^{3} \frac{1}{2} \oint_{D_i} \dot{\boldsymbol{r}}_i^{\mathrm{T}}(x_i,t)\dot{\boldsymbol{r}}_i(x_i,t)\,\mathrm{d}m_i + \frac{1}{2}\oint_{D_2} (\dot{T}_2(x_2,t))^2\,\mathrm{d}m_2, \tag{26}$$

where the last term is due to the torsional motion of Link 2. Using the relationship for the time derivative in Eq. (23), the kinetic energy can be separately rewritten as

$$\mathscr{T} = \mathscr{T}_0 + \mathscr{T}_1 + \mathscr{T}_2 + \mathscr{T}_3 + \mathscr{T}_4, \tag{27}$$

where

$$\mathscr{T}_0 = \frac{1}{2}J_1\dot{\theta}_1^2,$$
$$\mathscr{T}_1 = \frac{1}{2}\sum_{i=2}^{3} \boldsymbol{k}_0 \cdot \mathrm{II}_i \cdot \boldsymbol{k}_0\dot{\theta}_1^2,$$
$$\mathscr{T}_2 = \sum_{i=2}^{3} \dot{\theta}_1\boldsymbol{k}_0 \cdot \oint_{D_i} (\boldsymbol{r}_i \times \boldsymbol{j}_i)\dot{y}_i(x_i,t)\,\mathrm{d}m_i,$$
$$\mathscr{T}_3 = \frac{1}{2}\sum_{i=2}^{3} \oint_{D_i} (\dot{y}_i(x_i,t))^2\,\mathrm{d}m_i,$$
$$\mathscr{T}_4 = \frac{1}{2}\oint_{D_2} (\dot{T}_2(x_2,t))^2\,\mathrm{d}m_2.$$

The first three terms of Eq. (27) can be obtained by the inner product between $\boldsymbol{H}_\delta$ and the angular velocity of the rigid body. $\mathscr{T}_0$ is the kinetic energy from the rotation of rotor and $\mathscr{T}_1$ is the kinetic energy from the rigid rotation of robot. $\mathscr{T}_2$ is the kinetic energy due to the momentum transfer between modal angular momentum and rigid body angular momentum. If $\mathscr{T}_2$ is zero, there is no way of energy transfer between elastic motion and rigid motion. $\mathscr{T}_3$ and $\mathscr{T}_4$ are the modal kinetic energy only from elastic motion. Rewriting $y_2(x_2,t)$ and $y_3(x_3,t)$ using modal co-ordinates in Eq. (13) leads to

$$\begin{aligned}
\mathscr{T}_2 &= \sum_{i=2}^{3}\left[\dot{\theta}_1\boldsymbol{k}_0\cdot\oint_{D_i}(\boldsymbol{r}_i\times\boldsymbol{j}_i)\left(\sum_{i=1}^{m}\phi_{ij}(x_i)\dot{z}_j(t)\right)\mathrm{d}m_i\right],\\
\mathscr{T}_3 &= \frac{1}{2}\sum_{i=2}^{3}\left[\oint_{D_i}\left(\sum_{j=1}^{m}\phi_{ij}(x_i)\dot{z}_j(t)\right)^2\mathrm{d}m_i\right],\\
\mathscr{T}_4 &= \frac{1}{2}\oint_{D_2}\left(\sum_{j=1}^{m}\eta_j(x_2)\dot{z}_j(t)\right)^2\mathrm{d}m_2.
\end{aligned}\tag{28}$$

If we neglect gravity potential energy, the unique potential energy will be caused by the elastic potential energy such that

$$\mathscr{V} = \frac{1}{2}\sum_{i=2}^{3}\int_0^{L_i} EI_i(y_i''(x_i,t))^2\,\mathrm{d}x_i + \frac{1}{2}\int_0^{L_2} GJ_2(T_2'(x_2,t))^2\,\mathrm{d}x_2.\tag{29}$$

The first and the second terms of Eq. (29) are the strain energy from the bending and the torsional vibrations, respectively. Again, applying the modal co-ordinates to Eq. (29), we get

$$\mathscr{V} = \frac{1}{2}\sum_{i=2}^{3}\int_0^{L_i} EI_i\left(\sum_{j=1}^{m}\phi_{ij}''(x_i)z_j(t)\right)^2\mathrm{d}x_i + \frac{1}{2}\int_0^{L_2} GJ_2\left(\sum_{j=1}^{m}\eta_j'(x_2)z_j(t)\right)^2\mathrm{d}x_2.\tag{30}$$

Non-conservative work from joint torque is formulated as

$$\delta\mathscr{W} = \delta\theta_1\cdot\tau_1.\tag{31}$$

Let us define the Lagrangian $\mathscr{L} := \mathscr{T} - \mathscr{V}$ so that the equations of motion can be obtained from the Lagrangian dynamic formulation as

$$\frac{\mathrm{d}}{\mathrm{d}t}\left(\frac{\partial\mathscr{L}}{\partial\dot{q}_i}\right) - \frac{\partial\mathscr{L}}{\partial q_i} = \tau_i,\quad i = 1,\ldots,m+1,\tag{32}$$

where q_i is the ith element of generalized co-ordinate which is made up of

$$\boldsymbol{q} = [\theta_1\ z_1\ z_2\cdots z_m]^{\mathrm{T}} = [\theta_1\ \boldsymbol{z}^{\mathrm{T}}]\in\mathbb{R}^{m+1}.$$

It is satisfied that $\tau_i = 0,\ i = 2,\ldots,m+1$, since there is no input to the direction of modal co-ordinates. Applying kinetic and potential energies in Eqs. (27) and (30) to the Lagrangian $\mathscr{L}$, we have symbolic equations of motion based on the system mode approach as follows:

$$\begin{bmatrix}\boldsymbol{M}_{rr} & \boldsymbol{M}_{rf}\\ \boldsymbol{M}_{fr} & \boldsymbol{M}_{ff}\end{bmatrix}\begin{bmatrix}\ddot{\theta}_1\\ \ddot{\boldsymbol{z}}\end{bmatrix} + \begin{bmatrix}C_{rr} & \boldsymbol{C}_{rf}\\ \boldsymbol{C}_{fr} & \boldsymbol{0}\end{bmatrix}\begin{bmatrix}\dot{\theta}_1\\ \dot{\boldsymbol{z}}\end{bmatrix} + \begin{bmatrix}0 & \boldsymbol{0}\\ \boldsymbol{0} & \boldsymbol{K}_{ff}\end{bmatrix}\begin{bmatrix}\theta_1\\ \boldsymbol{z}\end{bmatrix} = \begin{bmatrix}\tau_1\\ \boldsymbol{0}\end{bmatrix},\tag{33}$$

where the bold characters stand for vector quantities and the normal characters for scalar quantities. The inertia matrix contains information about the angular momentum and kinetic energy. Each term of the inertia matrix is

$$\begin{aligned}
&M_{rr} = J_1 + \boldsymbol{k}_0 \cdot (\mathrm{II}_2 + \mathrm{II}_3) \cdot \boldsymbol{k}_0 \in \mathbb{R},\\
&\boldsymbol{M}_{rf} = [h_1, \ldots, h_m] \in \mathbb{R}^{1\times m},\\
&\quad \text{where } h_j \triangleq \sum_{i=2}^{3} \left[\oint_{D_i} \boldsymbol{k}_0 \cdot (\boldsymbol{r}_i \times \boldsymbol{j}_i)\phi_{ij}(x_i)\, \mathrm{d}m_i \right], \quad j = 1, \ldots, m,\\
&\boldsymbol{M}_{fr} = \boldsymbol{M}_{rf}^{\mathrm{T}} \in \mathbb{R}^{m\times 1},\\
&\boldsymbol{M}_{ff} = \boldsymbol{I}_m \in \mathbb{R}^{m\times m},
\end{aligned} \tag{34}$$

where $\boldsymbol{I}_m$ is an m-dimensional identity matrix. We utilize the orthogonality relation in Eq. (20) for removing the off-diagonal elements in $\boldsymbol{M}_{ff}$. M_{rr} is the inertia for rotation of joint 1 centered at Z_0-axis. $\boldsymbol{M}_{rf}$ is the coupled inertia. All the elements of $\boldsymbol{M}$ are constant except M_{rr}; M_{rr} contains flexure variables, but usually it is assumed constant by the linearization. $\boldsymbol{C}$ is arranged to satisfy the skew symmetry of $\dot{\boldsymbol{M}} - 2\boldsymbol{C}$ [19]. Finally, the stiffness matrix is simply given by

$$\boldsymbol{K}_{ff} = \mathrm{diag}\{\omega_1^2, \omega_2^2, \ldots, \omega_m^2\}, \tag{35}$$

where ω_j is the jth modal frequency from the analysis of the system mode. The constrained vibration equation is always given in a simply decomposed form:

$$\ddot{\boldsymbol{z}} + \boldsymbol{K}_{ff}\boldsymbol{z} = \boldsymbol{0}$$

by fixing $\theta_1 \equiv 0$.

4. Accessibility and identifiability

The accessibility condition in a physical plant is the same no matter what method we may describe the dynamics with. In this context, the discussion about the conditions and the physical meaning for the accessibility is made based on the dynamic equation derived in the previous section. As the duality with the accessibility, the identifiability is also defined and examined.

Suppose that the actuation and sensing take place only at joint 1. Applying the same assumptions that were made in Eq. (4), $\boldsymbol{M}$ is reduced to be constant and the Coriolis and centripetal force are negligible. By combining the upper part with the lower part of Eq. (33), we obtain an equation associated with the joint torque and system modes of vibration as

$$(\boldsymbol{I} - M_{rr}^{-1}\boldsymbol{M}_{fr}\boldsymbol{M}_{rf})\ddot{\boldsymbol{z}} + \boldsymbol{K}_{ff}\boldsymbol{z} = -M_{rr}^{-1}\boldsymbol{M}_{fr}\tau_1, \tag{36}$$

where M_{rr} is always positive, and so is M_{rr}^{-1}. Eq. (36) displays the same form as the fast subsystem of the singularly perturbed model [20]. If we define $u_1 \triangleq M_{rr}^{-1}\tau_1$, u_1 becomes a new control input. Through the coupled inertia $\boldsymbol{M}_{fr}$, u_1 controls the dynamics of vibration. In this point of view, $\boldsymbol{M}_{fr}$ acts as the AIC vector. The explicit form of the jth element of $\boldsymbol{M}_{fr}$, that is h_j, in Eq. (34) can be

rewritten as

$$h_j = \sum_{i=2}^{3} \left[\oint_{D_i} s_i(x_i)\phi_{ij}(x_i)\,\mathrm{d}m_i \right], \tag{37}$$

where $s_i(x_i) = \boldsymbol{k}_0 \cdot (\boldsymbol{r}_i \times \boldsymbol{j}_i)$ is the normal distance from the axis of rotation to a robot's body point; refer to Fig. 3 for graphical definition. Geometrically it is satisfied that

$$s_2(x_2) = x_2 \sin\theta_2, \quad s_3(x_3) = L_2 \sin\theta_2 + x_3 \sin(\theta_2 + \theta_3). \tag{38}$$

From Eq. (37), h_j is the first moment conceptually, where $s_i(x_i)$ is the length of arm from $\boldsymbol{k}_0$-axis, and $\phi_{ij}(x_i)$ acts as the physical quantity like the distributed linear force. According to Eq. (25), the projected angular momentum due to the pure elastic motion can be written as

$$\boldsymbol{k}_0 \cdot \boldsymbol{H}_\delta = \sum_{j=1}^{m} h_j \dot{z}_j(t), \tag{39}$$

where h_j is the weighting coefficient of the angular momentum caused by the jth mode. We call h_j as the jth modal angular momentum coefficient (MAMC). This means $\boldsymbol{M}_{fr}$ consists of MAMCs of all the vibration modes. If h_j happens to be zero at the given configuration, there is no contribution to the system's angular momentum in the $\boldsymbol{k}_0$ direction by the jth vibration mode. If the magnitude of h_j is large, the contribution of the jth mode to the angular momentum is also increased. The inner product of $\dot{\theta}_1\boldsymbol{k}_0$ and $\boldsymbol{H}_\delta$ results in the kinetic energy $\mathscr{T}_2$. That $h_j = 0$ means in a sense no momentum transfer between joint angular motion and the jth vibration mode, and the vibratory motion and angular rotation are appearing indifferent to each other.

Theorem 1. *If the jth element of $\boldsymbol{M}_{fr}$ (that is, MAMC of the jth mode) is zero, the jth vibration mode in Eq.* (36) *is not accessible by the input torque at the given configuration. Otherwise, the jth mode is accessible at the configuration.*

Proof. Consider that the jth element of $\boldsymbol{M}_{fr}$ is zero such that

$$\boldsymbol{M}_{fr} = [h_1 \ \cdots \ h_{j-1} \ 0 \ h_{j+1} \ \cdots \ h_m]^{\mathrm{T}}.$$

Then, the jth row and column of $\boldsymbol{M}_{fr}\boldsymbol{M}_{rf}$ also become zero, which yields the jth modal equation to be

$$\ddot{z}_j + \omega_j^2 z_j = 0. \tag{40}$$

This shows that the jth modal equation in Eq. (36) is a pure oscillator; this mode is completely isolated from the input, as well as from the other coupled vibration modes. If h_j is not zero, the control input can access the jth vibration mode through h_j. We can expect that the accessibility be increased as the magnitude of h_j is larger. This concludes the proof. □

Following the same lines as with accessibility, the identifiability condition can be derived by investigating the following equation:

$$(M_{rr} - \boldsymbol{M}_{rf}\boldsymbol{M}_{fr})\ddot{\theta}_1 + \boldsymbol{M}_{rf}\boldsymbol{K}_{ff}\boldsymbol{z} = \tau_1, \tag{41}$$

which is obtained by plugging the lower part into the upper part in Eq. (33). From the above equation, the second term on the left side is the stiffness force interacting with the joint motion, and $\boldsymbol{M}_{rf}$ determines the influence of the stiffness force.

Theorem 2. *Consider the system in Eq.* (41) *with feedback control from the joint measurements such that*

$$\tau_1 = -K_p\theta_1 - K_v\dot{\theta}_1. \tag{42}$$

If the jth element of $\boldsymbol{M}_{rf}$ (*that is*, h_j) *is zero*, *the jth mode cannot be identified by the joint sensor at the given configuration. Otherwise*, *the jth mode is identifiable by the joint sensor at the configuration.*

Proof. Introducing control input in Eq. (42) into Eq. (41), it becomes

$$(M_{rr} - \boldsymbol{M}_{rf}\boldsymbol{M}_{fr})\ddot{\theta}_1 + K_v\dot{\theta}_1 + K_p\theta_1 = -\boldsymbol{M}_{rf}\boldsymbol{K}_{ff}\boldsymbol{z}, \tag{43}$$

which implies a stable joint feedback system perturbed by the stiffness force on the right-hand side of the equation. Suppose that the MAMC of the jth mode be zero. Then, from Theorem 1, z_j will be sinusoidal for a non-zero initial condition. The stiffness force from the jth mode is always filtered by $\boldsymbol{M}_{rf}$ before acting on the joint dynamics in Eq. (43). If we remember the previous assumption that all the system modes are distinct, the portion of the stiffness force from the jth mode will be sifted through $\boldsymbol{M}_{rf}$. In a stable linear system, a sinusoidal output with a certain frequency will be observed only if there is a sinusoidal input with the same frequency. In the light of this fact, the joint encoder will never exhibit the component of the jth modal frequency for zero h_j. For non-zero h_j, the jth oscillation mode will appear in the joint response, even though it is damped somewhat due to the joint feedback. □

4.1. Numerical example

We illustrate an example for calculating MAMCs using the system mode method. Consider a 3-D two-link flexible robot whose physical parameters are summarized in Table 1. We do not consider the flexibility of the link in the direction of the gravity. First, we solve the eigenvalue

Table 1
Physical parameters

Contents	Symbol	Value
Length of Link 2	L_2	0.52 (m)
Length of Link 3	L_3	0.52 (m)
Mass of Link 2	M_2	0.44 (kg)
Mass of Link 3	M_3	0.16 (kg)
Mass of elbow actuator	M_c	1.62 (kg)
Mass of lumped tip	M_{tip}	0.29 (kg)
Stiffness of Link 2	EI_2	24.4 (N m^2)
Stiffness of Link 3	EI_3	6.35 (N m^2)

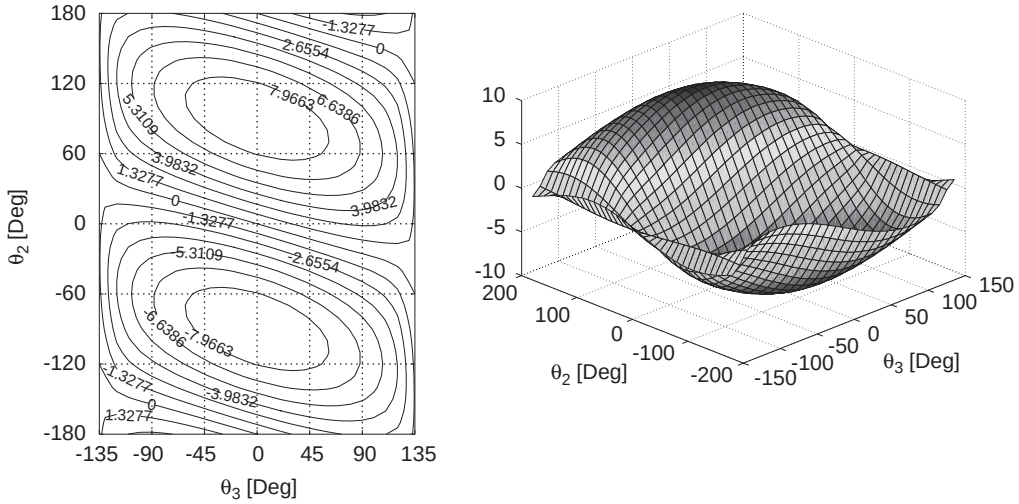

(a) Contour plot (b) 3-D plot

Fig. 4. Modal angular momentum coefficient: the first mode. (a) Contour plot; (b) 3-D plot.

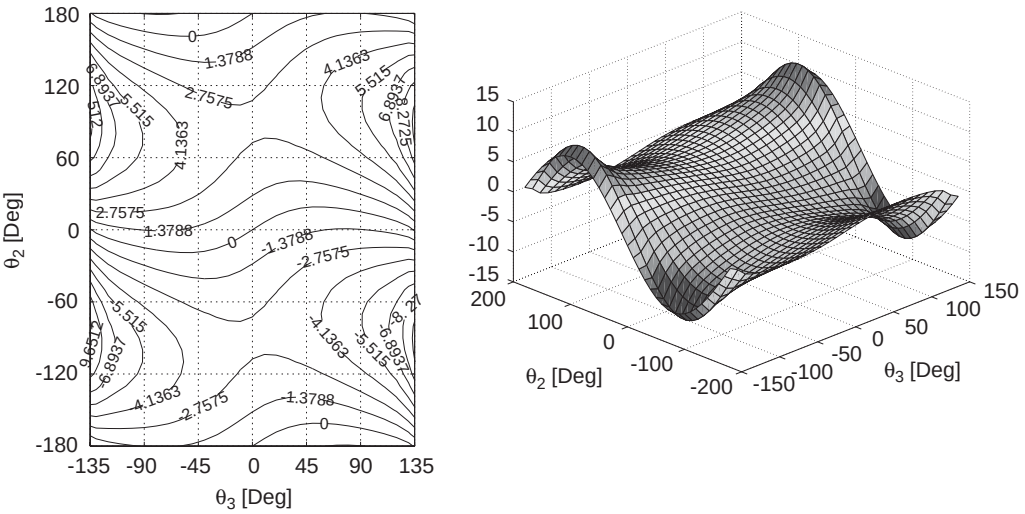

(a) Contour plot (b) 3-D plot

Fig. 5. Modal angular momentum coefficient: the second mode. (a) Contour plot; (b) 3-D plot.

problem using Eqs. (17) and (18). The solutions are plugged into Eq. (13) to obtain system mode shapes. Then, we compute MAMCs numerically following Eq. (37). Repeat the procedure by changing configurations of the robot gradually. Figs. 4 and 5 show the MAMCs of the first and the second system modes magnified 10 times. They vary from configuration to configuration. One can notice singular configurations where the MAMCs become zero. At those configurations, one

Fig. 6. POSTECH flexible robot: experimental system.

or all of the vibration modes cannot be accessed by τ_1. At a glance, as Link 2 is more directed to $\boldsymbol{k}_0$, the MAMCs tend to be smaller. The configurations close to singular lines correspond to the weakly accessible configurations. In the modal feedback control [21,22], the signs of the AICs are greatly important to the stability. In our terminology, the MAMCs will have the same meaning as the AICs. At weakly accessible configurations, the signs of the MAMCs might be estimated wrong in sign due to inexact modelling of kinematic and dynamic parameters, external disturbances, and measurement errors. The reverse feedback, no matter how small it may be, will cause the instability. The need for robust control in the weakly accessible configurations stems from these reasons, so the present control system is a good test plant for verifying the robustness of modal feedback controllers.

According to Figs. 4 and 5, at $(\theta_2, \theta_3) = (0^\circ, 0^\circ)$ and $(\theta_2, \theta_3) = (180^\circ, 0^\circ)$, the first and the second modes are inaccessible simultaneously. As for the first mode, the maximum magnitude of the MAMC shows at $(\theta_2, \theta_3) = (\pm 90^\circ, 0^\circ)$, and as for the second mode, the maximum magnitude of the MAMC will be at $(\theta_2, \theta_3) = (\pm 90^\circ, 180^\circ)$. If we remind the geometric structure of robot in mind, MAMCs have the following relations:

$$h_j(-\theta_2, -\theta_3) = -h_j(\theta_2, \theta_3)$$

and

$$h_j(\pi - \theta_2, -\theta_3) = h_j(\theta_2, \theta_3),$$

which are evident from Eqs. (37) and (38) without difficulty. According to the definition in Eq. (37), the modal angular momentum strongly depends on the mass distribution and the link

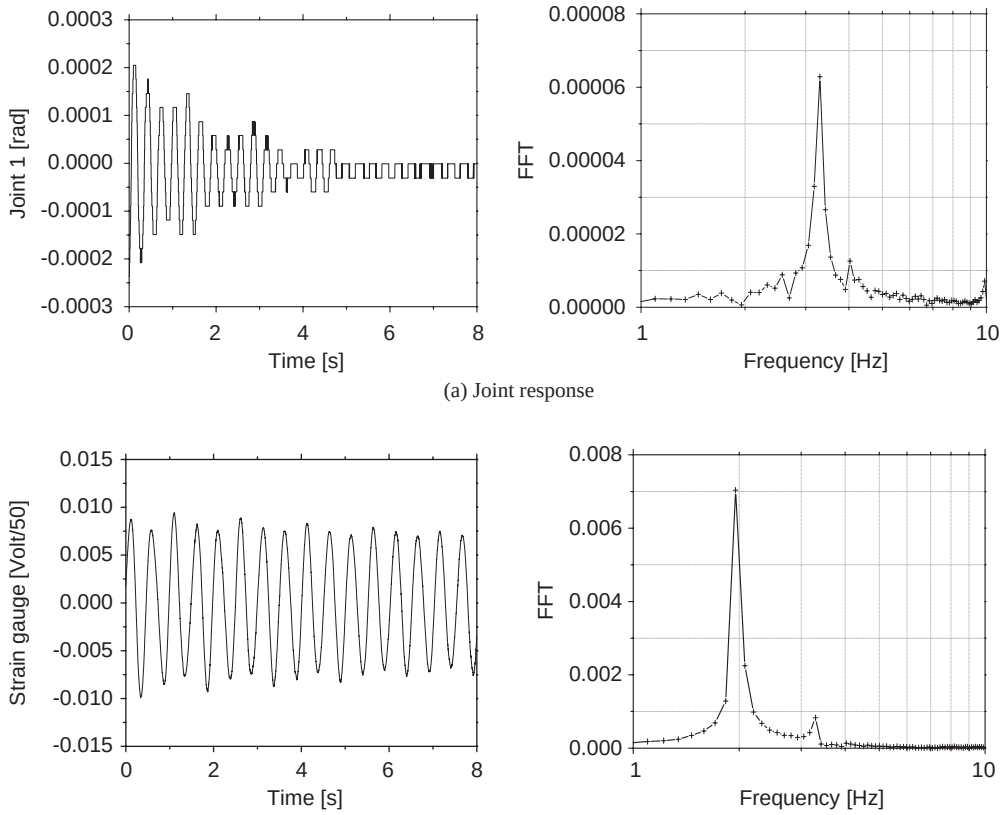

(a) Joint response

(b) Strain gauge response

Fig. 7. Impulse response at (C1): the first mode is unidentifiable. (a) Joint response; (b) strain gauge response.

configurations of the robot. The position of lumped masses and the addition of the payload mass will change the modal angular momentum. This implies that the modal angular momentum can be effectively changed by varying those parameters. Many of the previous researches on the controllability of the flexible robots and controllability related with flexible payloads may be put into the same category: the analysis of modal angular momentum.

In the foregoing discussion, the priority of the selection of the arm configuration for horizontal rotation lies in guaranteeing the satisfactory amount of accessibility. If it is satisfied, the next consideration would be the minimization of the rotational inertia M_{rr}. This is because the smaller M_{rr} reduces the total cost of energy and increases the speed of tasks. Since the rigid body inertia M_{rr} in Eq. (34) depends on the robot's geometry, we can take optimal configuration that minimizes M_{rr} as well as guarantees the sufficient accessibility for every the significant mode.

5. Experimental results

We performed experiments to justify the theoretical results. The experimental robot is shown in Fig. 6. Its physical parameters are the same as in Table 1. The angle of joint 1 was measured by

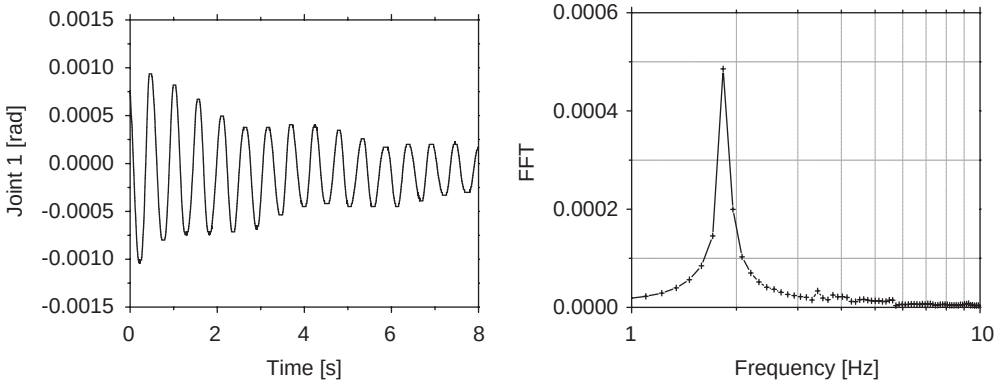

(a) Joint response

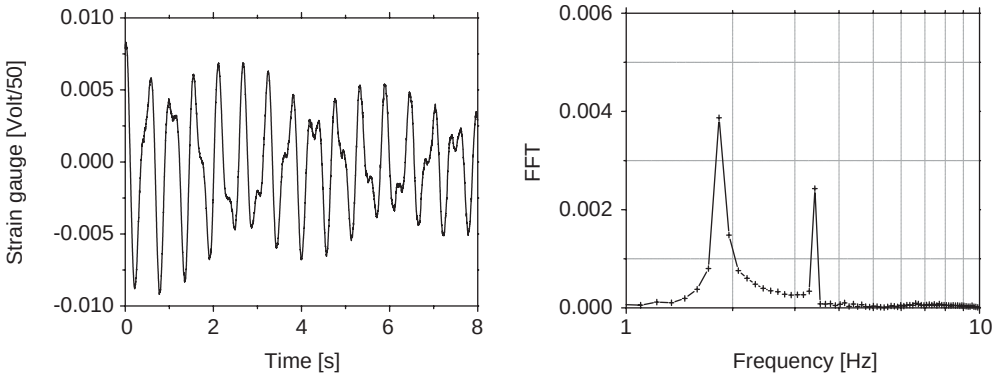

(b) Strain gauge response

Fig. 8. Impulse response at (C2): the second mode is unidentifiable. (a) Joint response; (b) strain gauge response.

optical encoder and the elastic vibration was measured by strain gauges at each side of elastic links. Since the test of the accessibility might be affected by the performance of the applied controller, we conducted the experiments on the identifiability, rather than on the controllability. Initially, we excited all the modes of vibration by exerting an impulse at the tip of robot with a hammer. Then we recorded the responses measured by strain gauges and joint encoder simultaneously. We checked the identifiability at three different configurations using the maps in Figs. 4 and 5:

(C1) $(\theta_2, \theta_3) = (-24^\circ, 85^\circ)$, where h_1 is zero,
(C2) $(\theta_2, \theta_3) = (18^\circ, 81^\circ)$, where h_2 is zero, and
(C3) $(\theta_2, \theta_3) = (50^\circ, 40^\circ)$, where both h_1 and h_2 are non-zero.

There are two dominant natural frequencies for those configurations; they are 1.98 and 3.26 Hz at (C1), 1.95 and 3.38 Hz at (C2), and 1.76 and 4.25 Hz at (C3). At each configuration, the robot was made to stand still by imposing high servo gains at joints 2 and 3. To exclude the interaction with the vertical vibration, a modal feedback vibration controller [20] was activated to suppress

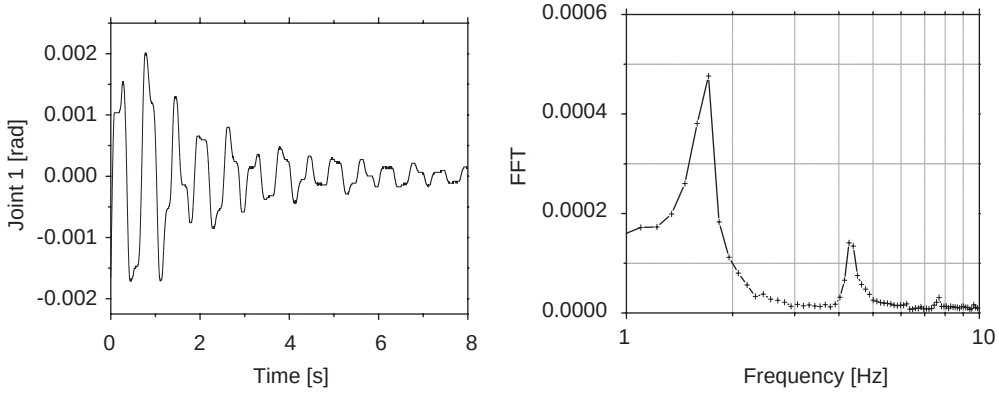

(a) Joint response

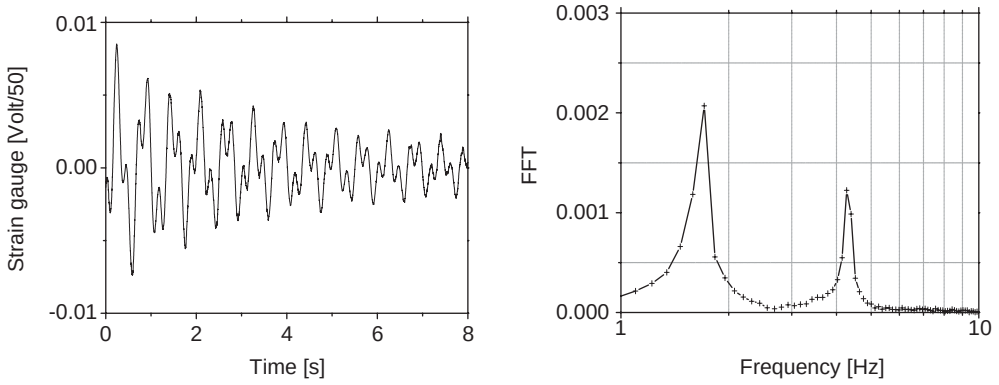

(b) Strain gauge response

Fig. 9. Impulse response at (C3): the first and second modes are identifiable. (a) Joint response; (b) strain gauge response.

the vertical vibration, while we tested the identifiability of the horizontal vibration. At joint 1, the following gains were applied to PD joint feedback in Eq. (42):

$$K_p = 350, \quad K_v = 3.8.$$

Since the proportional gain is considerably large, the elastic link extended from the rotary joint behaves almost like the constrained structure [16,23]. Figs. 7–9 show the test responses of joint 1 and the strain gauge attached at Link 3 at (C1)–(C3) cases. In order to clarify the frequency contents of the signal, each plot in time domain is presented together with its FFT plot. At configuration (C1) as shown in Fig. 7, the joint encoder could not measure the contents of the first mode (see Fig. 7(a)), even if the elastic links were oscillating dominantly with the first mode (see Fig. 7(b)). At configuration (C2), the second flexible mode is hardly identifiable by the joint encoder. Therefore, the joint could not measure the second mode (see Fig. 8(a)), even though the strain signals contained the second mode as shown in Fig. 8(b). Finally, Fig. 9 shows the responses at configuration (C3) where all the modes are identifiable. Both the joint and strain gauge signals

contain the first and the second modes simultaneously. Conclusively, the theoretical results of identifiability discussed in the previous section satisfies the experimental results well. Thanks to the dual relation, the accessibility of those configurations will be readily expected with the test results of the identifiability; at (C1) and (C2), the first and the second mode would be inaccessible, respectively, and at (C3), both modes would be accessible.

6. Concluding remarks

For the accessibility and the identifiability of the horizontal vibration in multi-link flexible robots, we developed the Lagrangian dynamics symbolically associated with the system mode vibration. Thereby, the meaning of each component of inertia matrix $\boldsymbol{M}$ was understood. Especially, we realized that

- the off-diagonal inertia $\boldsymbol{M}_{rf}$ (or $\boldsymbol{M}_{fr}$) consists of all the modal momentum coefficients,
- these coefficients indicate the amount of energy transfer between joint motion and the corresponding vibration modes, and
- if any element of the off-diagonal inertia becomes zero, those vibration modes will never be accessed and never be identified by the joint actuator and by the joint sensor, respectively.

We found that the modal angular momentum coefficients strongly depend on the mass distribution of robot components as well as the geometric configurations. When selecting a configuration for horizontal rotation task, we should guarantee the accessibility and the identifiability up to a sufficient level. In addition, we must consider such issues like minimization of rigid body inertia, robustness around weakly accessible region, and variation of modal angular momentum coefficients due to grasping payloads at the same time. To deal with these matters, the theoretical results addressed in this paper will provide basis knowledge.

References

[1] A. Konno, M. Uchiyama, Y. Kito, M. Murakami, Configuration-dependent vibration controllability of flexible-link manipulators, International Journal of Robotics Research 16 (1997) 567–576.
[2] L. Meirovitch, Dynamics and Control of Structures, Wiley, New York, 1989.
[3] M.J. Balas, Feedback control of flexible systems, IEEE Transactions on Automatic Control AC-23 (1978) 673–679.
[4] R. Piche, On the symmetrizability of structural control systems with noncolocated sensors and actuators, Transactions of the American Society of Mechanical Engineers Journal of Dynamic Systems, Measurement, and Control 112 (1990) 249–252.
[5] D.K. Miu, Physical interpretation of transfer function zeros for simple control systems with mechanical flexibility, Transactions of the American Society of Mechanical Engineers Journal of Dynamic Systems, Measurement, and Control 113 (1991) 419–424.
[6] P. Hughes, R.E. Skelton, Controllability and observability of linear matrix second-order systems, Journal of Applied Mechanics 47 (1980) 415–420.
[7] Z.-S. Liu, D.-J. Wang, H.-C. Hu, M. Yu, Measures of modal controllability and observability in vibration control of flexible structures, Journal of Guidance, Control, and Dynamics 17 (6) (1994) 1377–1380.
[8] C.N. Viswanathan, R.W. Longman, P.W. Likins, A degree of controllability definition: fundamental concepts and application to modal systems, Journal of Guidance and Control 7 (2) (1984) 222–230.

[9] S. Tosunoglu, S.-H. Lin, D. Tesar, Accessibility and controllability of flexible robotic manipulators, Transactions of the American Society of Mechanical Engineers Journal of Dynamic Systems, Measurement, and Control 114 (1992) 50–58.
[10] T. Zhou, J.W. Zu, A.A. Goldenberg, Vibration controllability of flexible robot-payload systems, in: Proceedings of the IEEE International Conference on Robotics and Automation, San Francisco, CA, 2000, pp. 1484–1489.
[11] Y. Shigang, Weak-vibration configurations for flexible robot manipulators with kinematic redundancy, Mechanism and Machine Theory 35 (2000) 165–178.
[12] W.J. Book, Recursive Lagrangian dynamics of flexible manipulator arms, International Journal of Robotics Research 3 (3) (1984) 87–101.
[13] P.C. Hughes, Modal truncation for flexible spacecraft, Journal of Guidance and Control 4 (3) (1981) 291–297.
[14] S.S.K. Tadikonda, T.G. Mordfin, T.G. Hu, Assumed modes method and articulated flexible multibody dynamics, Journal of Guidance, Control, and Dynamics 18 (3) (1995) 404–410.
[15] R.I. Milford, S.F. Asokanthan, Configuration dependent eigenfrequencies for a two-link flexible manipulator: experimental verification, Journal of Sound and Vibration 222 (2) (1999) 191–207.
[16] J. Cheong, Y. Youm, W.K. Chung, Investigation and comparison of possible boundary conditions and system vibration modes in two-link flexible manipulators, in: Proceedings of the American Society of Mechanical Engineers International Symposium on Advances in Robot Dynamics and Control, IMECE, CD-2, 2001.
[17] J. Cheong, Y. Youm, W. Chung, System mode approach for analysis of horizontal vibration of 3d two-link flexible manipulators, Journal of Sound and Vibration 268 (1) (2003) 49–70.
[18] P.C. Hughes, Modal identities for elastic bodies, with application to vehicle dynamics and control, Journal of Applied Mechanics 47 (1980) 177–184.
[19] C.C. de Wit, B. Siciliano, G. Bastin (Eds.), Theory of Robot Control, Springer, London, 1996.
[20] J. Cheong, Y. Youm, W.K. Chung, Joint tracking controller for multi-link flexible robot using disturbance observer and parameter adaptation scheme, Journal of Robotic Systems 19 (8) (2002) 401–417.
[21] W.B. Gevarter, Basic relations for control of flexible vehicles, American Institute of Aeronautics and Astronautics Journal 8 (4) (1970) 666–672.
[22] K. Huseyin, Vibrations and Stability of Multiple Parameter Systems, Noordhoff, Leiden, 1978.
[23] E. Garcia, D.J. Inman, Modeling of the slewing control of a flexible structure, Journal of Guidance 14 (4) (1991) 736–742.